Acta Oceanol. Sin., 2020, Vol. 39, No. 10, P. 129–139
https://doi.org/10.1007/s13131-020-1580-6
http://www.hyxb.org.cn
E-mail: hyxbe@263.net

Antibacterial and antiparasitic activities analysis of a hepcidin-like antimicrobial peptide from *Larimichthys crocea*

Libing Zheng[1, 3], Yuan Li[2], Jun Wang[1], Ying Pan[1], Jia Chen[1], Weiqiang Zheng[1], Longshan Lin[2*]

[1] State Key Laboratory of Large Yellow Croaker Breeding, Ningde 352103, China

[2] Third Institute of Oceanography, Ministry of Natural Resources, Xiamen 361005, China

[3] National and Provincial Joint Laboratory of Exploration and Utilization of Marine Aquatic Genetic Resources, School of Marine Science and Technology, Zhejiang Ocean University, Zhoushan 316022, China

Received 24 December 2019; accepted 14 February 2020

Abstract

As an economically important marine fish, the large yellow croaker *Larimichthys crocea* suffered from marine white spot disease caused by the ectoparasite *Cryptocaryon irritans* in recent years. This disease not only could result in physiological damage, but also lead to secondary bacterial invasion. Reports indicated some AMPs (antimicrobial peptides) were of antiparasitic activity to *C. irritans*. Hepcidin-like (*Lc-HepL*) was one of the significant differential expression genes excavated from the transcriptome following a challenge with *C. irritans*. In this study, we characterized this AMP's bioactivity based on the levels of mRNA and protein. After challenged by *C. irritans*, qRT-PCR showed *Lc-HepL* was significantly upregulated in six tissues, including gill, muscle, liver, head kidney and spleen during theront infection, trophont falling off, and secondary bacterial invasion stages, which implicated a role *Lc-HepL* played in the immune defense against *C. irritans* and secondary bacterial infection. Recombinant Lc-HepL (rLc-HepL) was induced and purified successfully. rLc-HepL exhibited antibacterial activity to certain bacteria in a dose- and time-dependent manners. Anti-*C. irritans* activity was explored for the first time and found it could cause the theronts membrane rupture and contents leakage. These results provided the first evidence that Lc-HepL had strong antiparasitic activity against marine fish ectoparasites *C. irritans* theronts. Together, data indicated that Lc-HepL might be an important component in the innate immune system against *C. irritans* and has the potential to be employed in future drug development.

Key words: *Larimichthys crocea*, *Cryptocaryon irritans*, hepcidin-like, antibacterial activity, antiparasitic activity

Citation: Zheng Libing, Li Yuan, Wang Jun, Pan Ying, Chen Jia, Zheng Weiqiang, Lin Longshan. 2020. Antibacterial and antiparasitic activities analysis of a hepcidin-like antimicrobial peptide from *Larimichthys crocea*. Acta Oceanologica Sinica, 39(10): 129–139, doi: 10.1007/s13131-020-1580-6

1 Introduction

AMPs (antimicrobial peptides) are the central components in the humoral immunity of the innate immune system involving in the first defense line, and are either induced after being infected by pathogens or stored in the secretory cells (Valero et al., 2020). AMPs present diverse sequences and structures (Mookherjee and Hancock, 2007) and exhibit strong activity to damage membranes, inhibit the proliferation of bacteria, kill bacteria directly (Patel and Akhtar, 2017), or interact with intracellular bio-macromolecules to disturb cell metabolism (Yeaman and Yount, 2003). In addition, some certain AMPs also have immunomodulatory properties (Valero et al., 2020; Oppenheim et al., 2003; Bowdish et al., 2006; Nicholls et al., 2010).

Hepcidin is a type of AMP with four disulfide linkages to take shape of a β-sheet structure. Hepcidin was firstly isolated from human blood in 2000 (Krause et al., 2000) and urine in 2001 (Park et al., 2001). Next, a mature peptide fragment was obtained from the gill of hybrid striped bass (*Morone chrysops* × *M. saxatils*), and the full-length cDNA was cloned (Shike et al., 2002). To date, increasing amounts of hepcidin were isolated and cloned from many fish species, such as *Danio rerio* (Shike et al., 2004), *Paralichthys olivaceus* (Hirono et al., 2005) and *Larimichthys crocea* (Wang et al., 2009), and the mature peptides contain 19–27 amino acid residues. Hepcidin from various sources has different resistance activity against pathogens (Krause et al., 2000; Shike et al., 2002; Wang et al., 2009), and a report showed the chemically synthetic hepcidin of *Tilapia mossambica* could also inhibit the growth of human fibrosarcoma cells (Chen et al., 2009). Hepcidin was likely to be the first defense line against pathogens invasion (Hirono et al., 2005; Lee et al., 2005), and it could coordinate with other AMPs to generate a synergistic antibacterial effect (Shi and Camus, 2006). Hepcidin of *L. crocea* (Lc-Hepc) exhibited broad-spectrum antibacterial activity and might interact with the signal molecules of pathogens through the electric charge effect to cause the formation of holes through which the contents leak (Cai, 2010).

In general, certain fish have multiple copies of hepcidin. Yang (2006) isolated two hepcidin sequences from the liver and gill of

Foundation item: The National Key Research and Development Program of China under contract No. 2018YFC1406302; the Local Science and Technology Development Project Guide by the Central Government under contract No. 2017L3019; the Development Project Guide by the Central Government under contract No. 2017L3019; the Technical Innovation Platform for Large Yellow Croaker under contract No. XDHT2018143A; the Major Special Projects of Fujian Province under contract No. 2016NZ0001.
*Corresponding author, E-mail: linlsh2005@126.com

Pagrosomus major after challenged by a bacterial mixture. Seven hepcidin sequences were identified from *Sparus macrocephlu*, and three hepcidin sequences found in *Oreochromis mossambicus* (Babitt et al., 2006). One of two hepcidin sequences of *P. olivaceus* was upregulated in the liver upon iron overload, while the other sequence was downregulated (Hirono et al., 2005).

Prior to our study, hepcidin and hepcidin-like genes were two differential expression AMPs excavated from the comparative liver transcriptome of *L. crocea* (Zheng et al., 2018). In this study, hepcidin-like was selected as the target gene, and we aimed to (1) detect the expression profiles after challenged by *C. irritans*; (2) construct a prokaryotic expression system with the pET-32a plasmid and host *Escherichia coli* BL21(DE3)pLysS, and induce expression of recombinant hepcidin-like (rLc-HepL); (3) purify the rLc-HepL; (4) analyze the antibacterial activity; and (5) analyze anti-*C. irritans* activity. The results might provide valuable data on the immune functions of Lc-HepL as a key component in the innate immune response against multiple pathogens.

2 Materials and methods

2.1 *Cryptocaryon irritans challenge experiment and tissue collection*

The challenge experiment was performed according to the pre-constructed procedure from our team (Niu, 2013). In brief, the tomonts of *C. irritans* were collected from the spontaneously infected *L. crocea* cultured at Ningde Marineland during an outbreak of marine white spot disease, and these tomonts were cultured at room temperature in sterile seawater (salinity of 32) for hatching theronts. The healthy *L. crocea* (temporarily reared for two weeks) were challenged with a dose of 26 665 theronts per fish (weight (85.5±15.1) g, body length (19.2±1.3) cm) in 500 L seawater for 4 h and then transferred to fresh seawater. Next, five individuals were randomly selected to dissect for tissue collection at 6 h, 1 d, 2 d, 3 d, 4 d, 5 d, 6 d, and 7d post-infection (pi). The healthy individuals were used as the control group. Tissues including gill, muscle, head kidney, liver, spleen and intestine were dissected, homogenized in RNAfixer (BioTek Corporation) immediately at 4°C overnight and then transferred to –20°C for total RNA extraction.

2.2 *Total RNA isolation and cDNA synthesis*

The detailed procedure of total RNA isolation was carried out according to the reference (Zheng et al., 2018). In short, the tissues were crushed in the RNAiso Plus (TaKaRa, Japan) and extracted with chloroform, nucleotide acid was precipitated for approximately 1 h with isopropyl alcohol at –20°C, and washed with 75% ethanol. The quantity and purity of the RNAs were tested by spectrophotometer (A260/A280). cDNAs were reverse transcribed using total RNA as templates with PrimerScript™ RT reagent and gDNA Eraser kit (TaKaRa, Japan) according to the protocol.

2.3 *Expression changes of Lc-HepL mRNA after challenged by C. irritans*

According to the cDNA sequence of *Lc-HepL*, a pair of primers, qHep-F/R (Table 1), were designed for quantitative real-time PCR (qRT-PCR) detection. β-actin was used as the internal control gene. The reactions were run on an ABI Quantitative 6 Flex system with SYBR Premix Dimer Eraser Kit (TaKaRa, Japan) following the established protocol. The detailed programs were used as the reference (Niu, 2013).

The relative expression level was quantified by the $2^{-\triangle\triangle Ct}$ method (Livak and Schmittgen, 2001). Each reaction was performed in triplicate, and all data were shown as the mean±SD (standard deviation of the mean). One asterisk indicated significant at $p<0.05$, and two asterisks indicated highly significant at $p<0.01$.

Table 1. The primers used in the experiments

Primers	Sequence (5′-3′)
qHep-F	CACATCCAACCATCAGACCAG
qHep-R	GAAGACAAATGAAGGCGAGCA
BHepL-F	CCGCAGGGCAGCCCTGCTAGATG
BHepL-R	CCGGAACCTGCAGCAGATACC
T7-prometer	TAATACGACTCACTATAGGG
T7-terminator	GCTAGTTATTGCTCAGCGG
β-actin-F	AAGCCAACAGGGAGAAGATGAC
β-actin-R	ACGACCAGAGGCATACA

2.4 *Construction of expression vector and induction of rLc-HepL*

2.4.1 *Construction of expression vector*

To amplify the sequence encoding mature peptide, specific primers BHepL-F/R (Table 1) were designed according to the sequence that introduced *EcoR* I/*Xho* I sites into the 5′ end respectively. PCR was performed in a 25 μL volume with Reaction Mix (TransGen, Beijing), and the products were refined by gel purification. The purified products and pET-32a were digested with enzymes *EcoR* I and *Xho* I (Thermo Scientific, USA), and the digested PCR products were sub-cloned into the pET-32a. Next, recombinant plasmids were transferred into the host competent cells of *E. coli* BL21(DE3)pLysS, selected with a LB agar plate containing 100 μg/mL ampicillin. The positive clones were selected to perform bacterial PCR and sequenced with T7 primers (Table 1). The positive clone containing the correct target sequence was stored in 25% (v/v) glycerinum at –80°C.

2.4.2 *Optimization of induction expression conditions*

The recombinant bacteria were cultured in fresh LB medium containing 0.5% glucose at 37°C, 180 r/min overnight. This solution was later inoculated into the same fresh medium at a 1:50 ratio and cultured at 37°C until the OD_{600} reached 0.6–0.7; isopropyl β-D-thiogalacto-pyranoside (IPTG) was added to final concentrations of 0.1, 0.3, 0.5, and 1.0 mmol/L to initiate induction at 37°C, 28°C and 18°C, respectively. Auto-induction in a simplified medium (Zhang, 2013) was explored in the study with induction time of 6 h at 37°C, 28°C and overnight at 18°C.

At the same time, initial OD_{600} values 0.1, 0.3, 0.5, 1.0, and induction expression for 1, 3, 5, 7, 9, 11 h were also explored to determine the optimal induction condition, respectively. Two hundred microliters (μL) of induction solution was taken out to be centrifuged at 5 000 g for 5 min, and the precipitates were prepared for sodium dodecyl sulfate polyacrylamide gel electrophoresis (SDS-PAGE) analysis.

2.5 *Capture and purification of rLc-HepL*

According to the above-mentioned optimum induction conditions, a large-scale (2 L) induction expression was performed. The induction solution was centrifuged at 12 000 r/min for 10 min at 4°C to harvest the cells, and the precipitates were resuspended in 500 mL pre-chilled Tris-HCl buffer (50 mmol/L Tris-HCl, 500 mmol/L NaCl, 20 mmol/L imidazole, pH 7.8). The mixture was sonicated with an ATS high pressure homogenizing ma-

chine (ATS Engineering Inc., Canada), centrifuged at 12 000 r/min for 30 min at 4°C to isolate the supernatant and precipitates, and they were analyzed by SDS-PAGE, respectively.

Throughout the detection process, the supernatant was filtered with a 0.22 μm filter membrane for purification by immobilized metal-chelating affinity chromatography (IMAC) mean. In brief, 15–25 mL sterile MilliQ water and Tris-HCl buffer were used to wash and equilibrate HisCap 6FF column (Smart-Lifesciences, Changzhou), respectively. The prepared supernatant was allowed to flow through the column by gravity at 4°C. The column was later washed with graded imidazole to remove nonobjective proteins and capture rLc-HepL through a UV detector in an AKTA Purifier 100 (GE Healthcare Life Sciences). All of the fluid collected from each elution peak was analyzed by SDS-PAGE.

Dialysis was used to remove high concentration imidazole which might influence the activity detection from the collected eluate containing pure rLc-HepL. The solution of interest was bathed in 50 mmol/L Tris-HCl buffer (50 mmol/L Tris-HCl, 50 mmol/L NaCl, pH 7.8) for 12 h at 4°C, and continually dialyzed in MilliQ water for 12 h at 4°C two times. The concentration was subsequently determined by the BCA method, and the eluate was finally freeze-dried.

The detailed procedure of Western blot analysis was based on previous research (Zheng et al., 2016). Following the Western blot transfer, the PVDF (polyvinylidene fluoride) membrane was blocked with 5% non-fat milk at room temperature for 2–3 h, incubated with anti-His mouse monoclonal antibody (abm, Canada) (diluted 1:1 000) overnight at 4°C, and continually bathed in goat anti-mouse IgG (H+L) horseradish peroxidase conjugated antibody (TransGen Biotech, China) (diluted 1:5 000) for 2 h at room temperature. After washed with PBST, the transformed stripe was dyed with a DAB Kit (Solarbio, China) according to the instructions and a picture was taken.

2.6 *Antibacterial activity of rLc-HepL*

2.6.1 *Antibacterial assays*

MIC (minimal inhibitory concentration) and MBC (minimal bactericidal concentration) were determined against a panel of microorganisms. In total, 13 types of bacteria were employed in the antibacterial tests, including Gram-positive *Bacillus subtilis*, *Staphylococcus aureus*, *Corynebacterium glutamicum*, *Micrococcus lysodeikticus*, and Gram-negative *E. coli*, *Pseudomonas fluorescens*, *Pseudomonas aeruginosa*, *Photobacterium damselae*, *Shigella flexneri*, *Aeromonas hydrophila*, *Vibrio harveyi*, *Vibrio alginolyticus* and *Vibrio Parahaemolyticus*. All non-marine bacteria were cultured in Muller-Hinton Broth (MHB), marine bacteria were cultured in saline peptone water (3% Tryptone, 3% NaCl, w/v) (Destoumieux et al., 1999).

A liquid growth inhibition assay on a 96-well flat-bottom tissue-culture plate was performed to determine the MIC as previously described (Niu, 2013; López-García et al., 2007; Lauth et al., 2005). rLc-HepL was gradient diluted to a concentration of 100–3.125 μmol/L with sterile MilliQ water. Logarithmic phase bacterial culture was washed with 10 mmol/L NaPB (68.4 mmol/L Na_2HPO_4, 31.5 mmol/L NaH_2PO_4), and suspended in working medium (MHB:NaPB=2:3) to a final OD_{600} of 0.003. Marine bacteria were suspended in saline peptone water to a final OD_{600} of 0.006. Next, 50 μL diluted rLc-HepL was mixed with 50 μL bacterial suspension. Samples without rLc-HepL or rTRX replacing rLc-HepL were used as blanks, respectively. After incubation for 24 h at 28°C, the MIC was calculated as a range between visible or no visible bacterial growth.

To determine the MBC, aliquots from the wells with no detectable growth were coated onto MHA and incubated overnight at 28°C or 37°C to assess viability. Each assay was performed in triplicate.

2.6.2 *Dose-dependent antibacterial activity*

According to the antibacterial spectrum results, *C. glutamicum* was chosen for the dose-dependent antibacterial tests. The bacterial suspension was adjusted to a final OD_{600} of 0.003 in working medium. Similarly, the final concentration range of rLc-HepL was 1.563–50 μmol/L. The mixtures were cultured for 3 h at 28°C, and 0.7 μL from each well was coated onto MHA and cultured at 30°C for 12–18 h, while rLc-HepL replaced by sterile MilliQ water or rTRX were used as the control, respectively. The colonies were counted, with the percentage of CFU (colony forming units) in the control group being treated as 100%, and the other groups were defined relative to the control group (Lauth et al., 2005).

2.6.3 *Kill-curve analysis*

Corynebacterium glutamicum and *P. damselae* were selected for studying the kill-curve as described previously (Niu, 2013; Supungul et al., 2008). Two-fold MBC concentration of rLc-HepL was incubated with the adjusted bacterial solution, rLc-HepL replaced by sterile MilliQ water or rTRX were used as controls, respectively. At various times, 0.7 μL of the mixture was taken from the well, coated on MHA, and incubated at 30°C for 12–18 h. The calculation method was the same as that mentioned above.

2.6.4 *SEM observation of antibacterial effect*

To observe the morphological changes on bacteria caused by rLc-HepL treatment, a SEM (scanning electron microscope) was employed in this study. *Corynebacterium glutamicum* and *P. damselae* were selected to represent the Gram-positive and Gram-negative bacteria, respectively. The bacteria were adjusted to 1×10^8 CUF/mL ($OD_{600}\approx1.0$) with working medium, and rLc-HepL was added to a final concentration of 50 μmol/L. rLc-HepL replaced by sterile MilliQ water or rTRX were used as controls, respectively. The mixture was incubated at 28°C, and samples were fixed with 2.5% glutaraldehyde at various times overnight at 4°C. All fixative solutions were washed with 0.01 mol/L PBS (pH 7.4), dehydrated in a graded ethanol series, freeze-dried, and gold sputtered. Prepared samples were observed in JSM-6 390 LV SEM.

2.7 *Antiparasitic activity observation of rLc-HepL with LM (light microscope)*

To preliminarily observe the antiparasitic activity of rLc-HepL, an antiparasitic assay was designed to determine the morphologic changes in *C. irritans* theronts treated with 40 μmol/L rLc-HepL. The theronts released from tomonts in 3 h were used to perform the test. Approximately 300 theronts were added to a 48-well plate containing 40 μmol/L rLc-HepL solution to a total volume of 1 mL at room temperature, and 200 μL of the mixture was fixed with 5.0% glutaraldehyde at various times at 4°C overnight, while rLc-HepL replaced by sterile MilliQ water or rTRX were used as controls, respectively. Prepared samples were observed on LM (LEICA ICC50 W, Germany).

3 Results

3.1 *The sequence analysis*

Lc-HepL consists of a 258 bp ORF encoding a peptide of 85 amino acids with eight cysteines in the mature peptide to form four disulfide linkages which was employed for antibacterial function. The putative peptide contains a conserve signal peptide, motif RENR. There were only two amino acids variation sites between *Lc-HepL* and *Lc-hepc*.

3.2 *Expression changes of Lc-HepL mRNA after C. irritans infection (Fig. 1)*

According to the sequence analysis, only two amino acids was different between hepcidin and hepcidin-like, but no available qRT-PCR primers were screened to identify the two variants, so we could only detect the overall expression changes. After challenged by *C. irritans*, the *Lc-HepL* mRNA was upregulated instantaneously to peak level in the gill at 6 h pi, which was one of the primary infected tissues, and recovered to the basal expression level from 46-fold (p<0.01) instantaneously at 1 d pi. In the intestine, upregulation occurred at 3 d pi, maximum expression was reached at 4 d pi when the level was 8.66-fold (p<0.01), and gradually returned to normal at 6 d pi. Secondly, highly significant expression peaks appearing at 7 d pi were found in such tissues as head kidney, spleen, liver and muscle, where the levels were 4.12-fold, 9.27-fold, 24.015-fold and 7.85-fold, respectively. In addition, the presence of expression peaks in the head kidney and muscle was instantaneous, while it was upregulated at 4 d pi and gradually reached the maximum expression in the liver. Therefore, as seen from the expression peaks, gill was the only tissue to reach a peak early in the infection, where the extent of upregulation was the greatest; intestine was the only tissue where the greatest upregulation occurred at 4 d pi when the trophonts of *C. irritans* were falling off; at 6–7 d pi, in the secondary bacterial infection phase, *Lc-HepL* mRNA was upregulated in the other four tissues. Therefore, the induction expression of *Lc-HepL* mRNA by *C. irritans* appeared to be a time-dependent and with instantaneous expression trend.

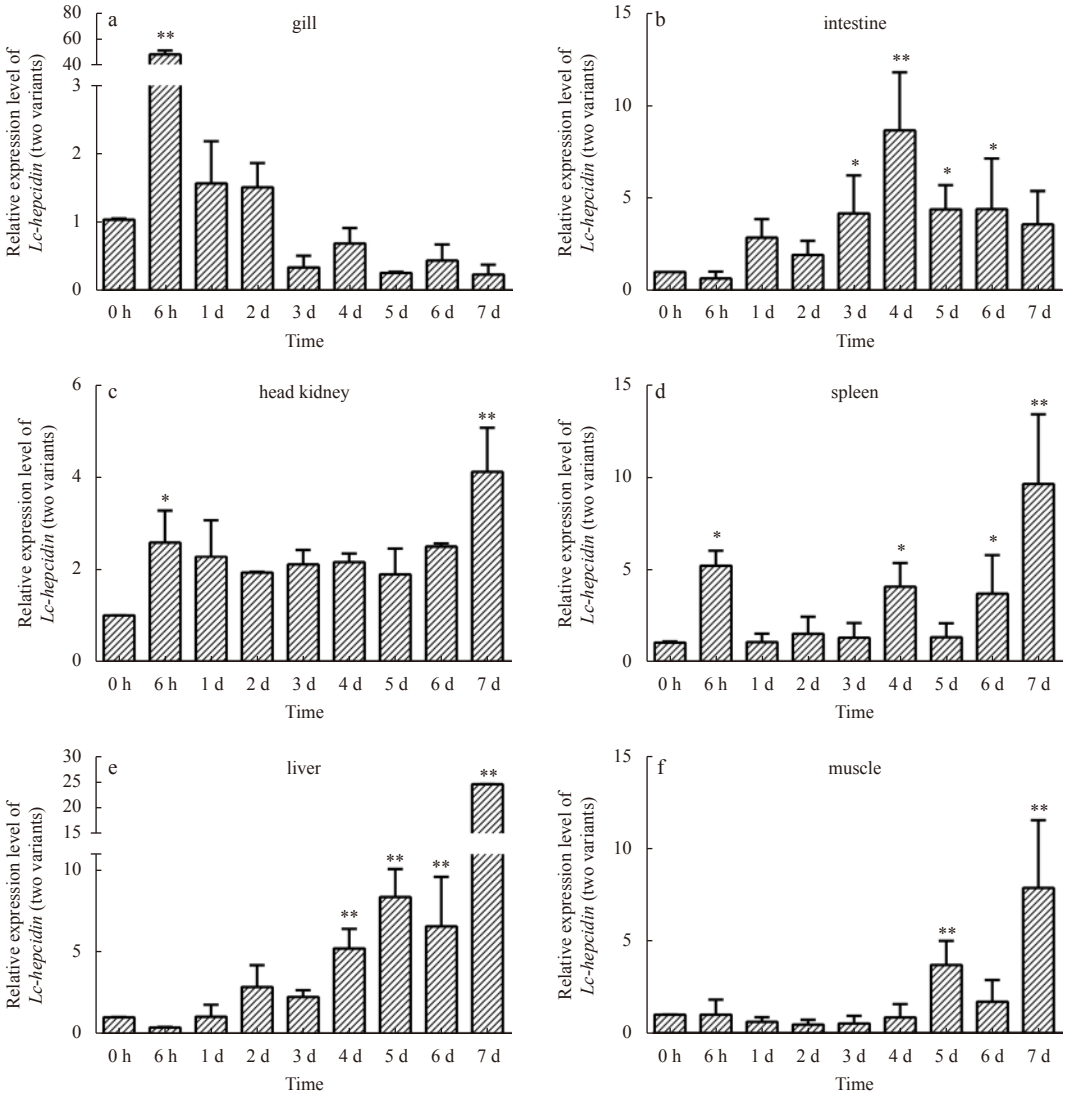

Fig. 1. The expression changes of *Lc-HepL* mRNA (two variants) in various tissues after challenged by *C. irritans* at various time points. Compared to the control group, one asterisk indicated significant difference (p<0.05), and two asterisks indicated highly significant differences (p<0.01).

3.3 *Capture of rLc-HepL*

3.3.1 *Optimization of induction expression conditions*

The induction results by various IPTG concentrations or auto-induction means were shown in Fig. 2. Compared to the blank group, the induced groups presented a distinct band at the position of 25 kDa, which was consistent with the expected size. As seen from the pictures, there were no visible differences among the various IPTG concentrations at the same induction temperature. Induction expression levels by IPTG or auto-induction appeared to have a positive correlation with the temperature. Therefore, 0.1 mmol/L IPTG or auto-induction at 37°C were sufficient.

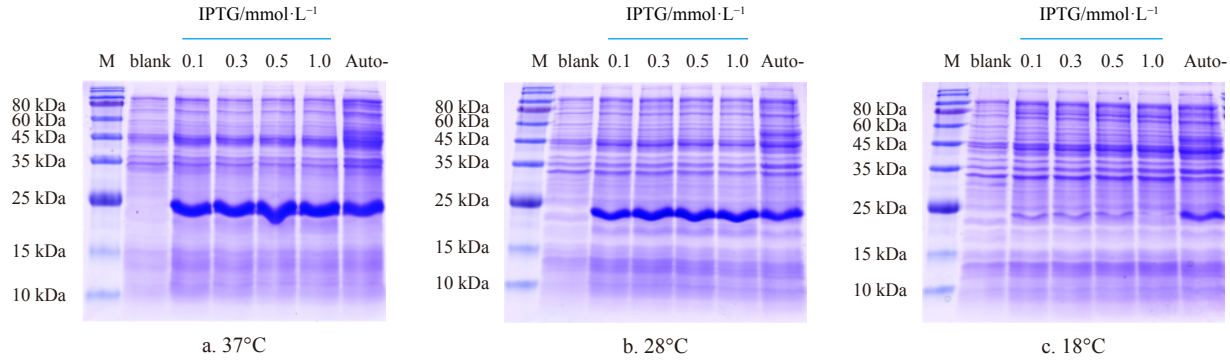

Fig. 2. SDS-PAGE analysis of rLc-HepL induction expression at different temperature by IPTG and auto-induction. M: protein molecular standard (TransGen Biotech, China); blank: total cellular extracts from *E. coli* BL21(DE3)pLysS containing recombinant plasmid before IPTG induction; Auto-: auto-induction method.

3.3.2 *Exploration of initial OD_{600}*

The induction expression results at various initial OD_{600} were shown in Fig. 3. With increasing of OD_{600} from 0.1 to 0.9, the expression level apparently decreased, namely the expression level appeared to have a negative correlation with the initial OD_{600}. Therefore, an initial OD_{600} of 0.1 was sufficient to induce rLc-HepL.

3.3.3 *Exploration of induction time*

SDS-PAGE analysis of rLc-HepL induction expression for different times was shown in Fig. 4. Within 7 h, the expression level increased as the time extended; from 7 h to 11 h, the expression level showed no visual difference. Therefore, 7 h induction was sufficient for rLc-HepL expressioin.

3.3.4 *Purification of rLc-HepL*

According to the explored induction conditions, a large-scale induction was carried out. Prior to purification, the expression form must be detected. Figure 5 showed that rLc-HepL existed both in the supernatants and inclusion bodies. During the purification process, the graded imidazole was used to remove the nonobjective protein contamination and capture pure rLc-HepL. The eluent containing pure rLc-HepL was dialyzed to remove the imidazole, and the concentration was 0.986 mg/mL.

3.3.5 *Western blot analysis*

The Western blot result was shown in Fig. 6, 6×His-tag was able to interact with the mouse monoclonal antibody. Thus, the purified rLc-HepL was adequate for the following tests.

3.4 *Antibacterial activity of rLc-HepL*

3.4.1 *MIC and MBC detection*

The antibacterial spectrum of rLc-HepL was shown in Table 2. The results showed rLc-HepL was highly active against certain

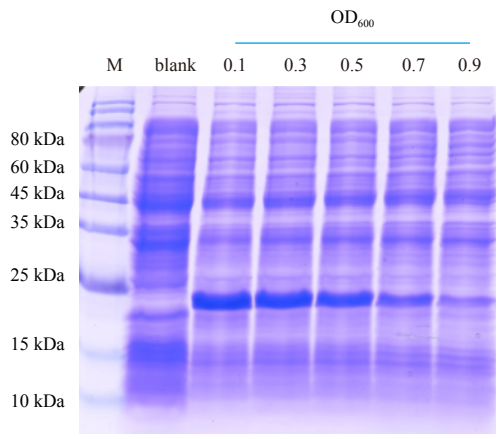

Fig. 3. SDS-PAGE analysis of rLc-HepL induction expression at different initial OD_{600} values. M: protein molecular standard (TransGen Biotech, China); blank: total cellular extracts from *E. coli* BL21(DE3)pLysS containing recombinant plasmid before IPTG induction.

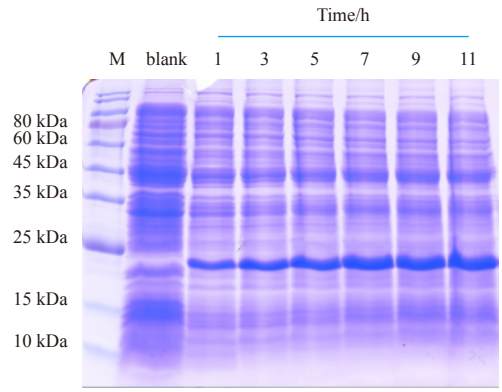

Fig. 4. SDS-PAGE analysis of rLc-HepL induction expression for different time. M: protein molecular standard (TransGen Biotech, China); blank: total cellular extracts from *E. coli* BL21(DE3)pLysS containing recombinant plasmid before IPTG induction.

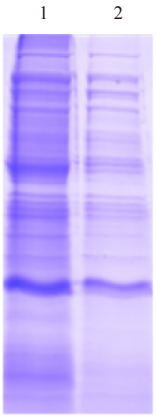

Fig. 5. The soluble analysis of rLc-HepL by SDS-PAGE. 1: The supernatant after ultrasonication; 2: the inclusion body after ultrasonication.

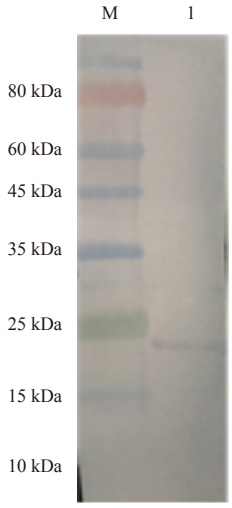

Fig. 6. Western blot analysis of rLc-HepL. M: protein molecular standard (TransGen Biotech, China); 1: Western blot analysis.

bacteria, including *C. glutamicum*, *M. lysodeikticus*, and *P. damselae*. These three bacteria were all susceptible to rLc-HepL (<3.125 μmol/L), while the MIC for other tested bacteria was >50 μmol/L. For these three bacteria, the MBC was either equal to or two times of the MIC.

3.4.2 *Dose-dependent antibacterial activity*

The *C. glutamicum* was incubated with rLc-HepL at 28°C for 3 h, and the relative percentage of CFU was shown in Fig. 7. Evidently, as the concentration of rLc-HepL increased, the survival rate decreased. In other words, the antibacterial activity of rLc-HepL to *C. glutamicum* appeared to be strictly dose-dependent.

3.4.3 *Kinetics of killing of C. glutamicum and P. damselae*

Figure 8 showed the survival rate of *C. glutamicum* and *P. damselae* upon exposure to rLc-HepL with 2-fold MBC at various times. Within 2 h, approximately 70% of the bacteria were killed. During the sampled times, the two bacteria had not been completely killed. In fact, the kinetics study showed that rLc-HepL killed the bacteria gradually and slowly.

3.4.4 *SEM observation on antibacterial effect to C. glutamicum*

Corynebacterium glutamicum, representing Gram-positive

Table 2. Antibacterial spectrum of rLc-HepL

Bacteria	CGMCC	MIC /μmol·L^{-1}	MBC /μmol·L^{-1}
Gram-positive bacteria			
Corynebacterium glutamicum	1.1886	<1.5625	1.5625–3.125
Micrococcus lysodeikticus	1.634	1.5625–3.125	3.125–6.25
Gram-negative bacteria			
Photobacterium damselae	Lab	<1.5625	<1.5625

Note: Lab represents the bacteria were stored in our laboratory.

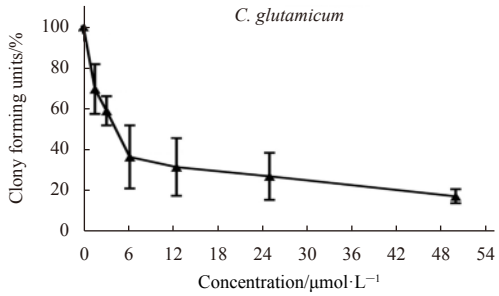

Fig. 7. Dose-dependent antibacterial activity of rLc-HepL.

bacteria, was treated to perform SEM, and the results were shown in Fig. 9. *Corynebacterium glutamicum* showed a smooth surface and dispersed over the microscopic field in the control groups. When treated by rLc-HepL, the bacteria were found aggregated and surrounded by floccule materials. A mass of *C. glutamicum* gathered gradually, and a small amount of floccule material appeared around part of the bacteria at 15 min (Fig. 9b); a larger amount of floccule material wrapped the bacteria after 30 min incubation, and the surface of the bacteria became rough with the appearance of processes indicating the development of content leakage; floccule materials grew gradually and formed into a honeycomb structure at 2 h (Figs 9c–e). All of these data indicated the antibacterial effect of rLc-HepL on *C. glutamicum* was already functioning at 15 min.

3.4.5 *SEM observation on antibacterial effect to P. damselae*

After treated with rLc-HepL, SEM observed the changes in *P. damselae,* and the result was shown in Fig. 10. *Photobacterium damselae* presented a smooth, clean surface and dispersed over the microscopic field when the cells were incubated with sterile MilliQ water or rTRX in the control group (Fig. 10a). After treated with rLc-HepL, the two obvious changes were the appearance of the flocculent structures and the aggregation of the bacteria. After incubation for 15 min, the surface became rough with the appearance of different extent processes, and the bacteria were covered by a small amount of floccule materials (Fig. 10b). Many *P. damselae* were found aggregated wrapped by a larger amount of floccule materials within 30 min after incubation, and some bacteria were disformed (Fig. 10c). The flocculent structures began to form into the honeycomb structure and coated onto the bacteria at 1 h incubation (Fig. 10d). Continuously, the honeycomb structure became highly significant at 2 h (Fig. 10e), but the number of misshapen bacteria did not increase from 1 h to 2 h.

3.5 *Antiparasitic activity of rLc-HepL*

The LM results of rLc-HepL effect on *C. irritans* theronts were shown in Fig. 11. Compared to the theronts with rounded bodies and clear cilia in the control group, there were no integral or detailed changes after incubation for 15 min (Fig. 11b). The visible

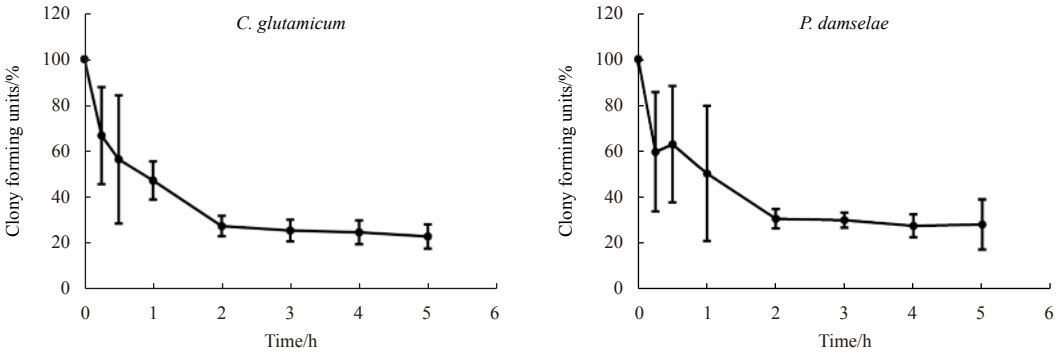

Fig. 8. Time-dependent antibacterial activity of rLc-HepL.

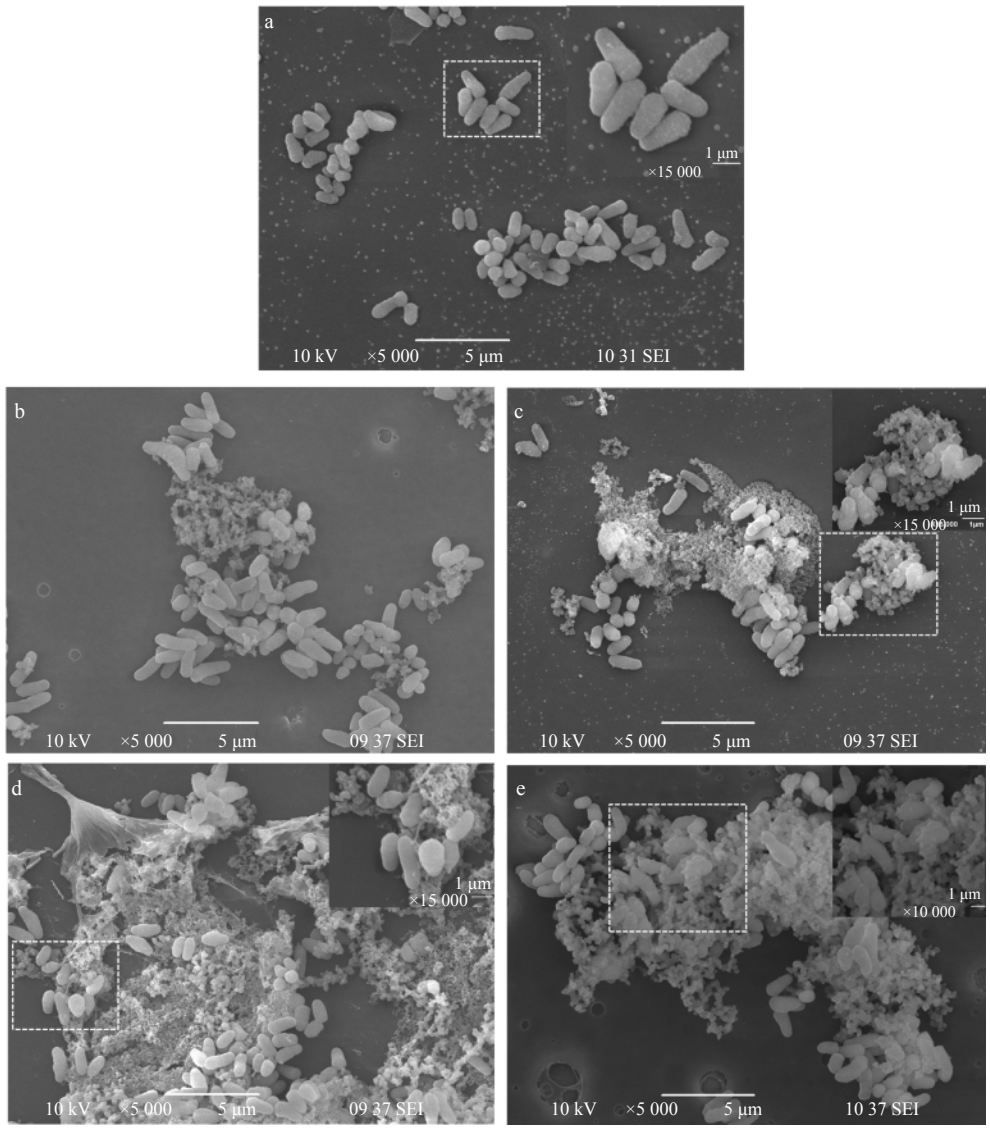

Fig. 9. SEM observation of *C. glutamicum* incubated with rLc-HepL. a. The control groups; and b–e. *C. glutamicum* treated for 15 min (b), 30 min (c), 1 h (d), 2 h (e), respectively.

changes began at 30 min, with some cilia no longer erect, instead lying down on the surface, and obvious processes appeared (Fig. 11c). The processes increased in number and size at different positions, which caused the cells disformed at 1 h (Fig. 11d). Similar damages continued, with the cells being completely deformed at 1.5 h, membrane ruptured at different positions causing contents leakage (Fig. 11e). These data indicated that rLc-HepL had antiparasitic activity on *C. irritans* theronts.

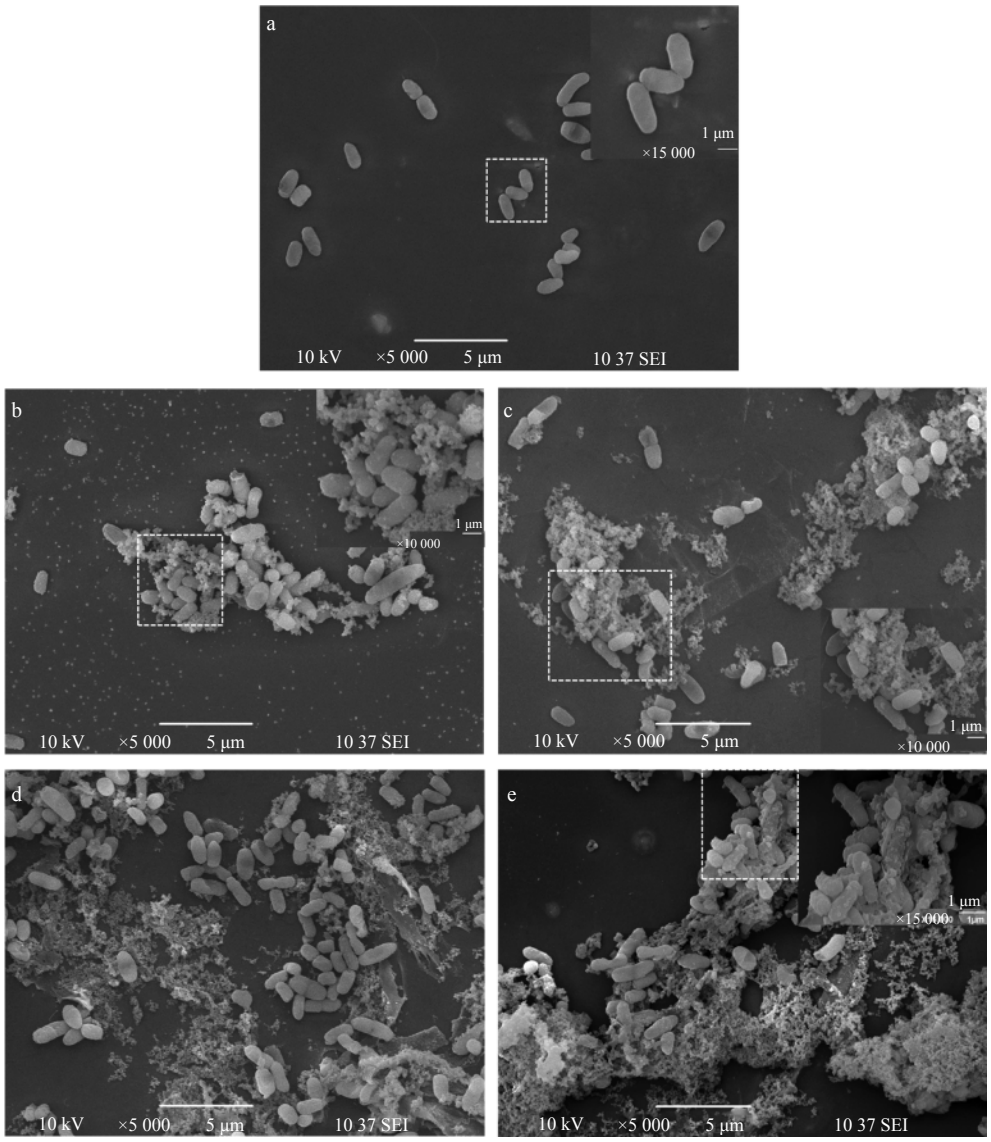

Fig. 10. SEM observation of *P. damselae* incubated with rLc-HepL. a. The control groups; and b–e. *P.damselae* treated for 15 min (b), 30 min (c), 1 h (d), 2 h (e), respectively.

4 Discussion

The signal peptide of hepcidin was highly conserved in fish, except for the zebrafish (Shike et al., 2004) and the channel catfish (Hu et al., 2007). The putative motif RENR was conserved in the *Lc-HepL* and *Lc-hepc* (Wang et al., 2009), which was different from the typical RX(K/R)R found in most other fish (Shike et al., 2002; Douglas et al., 2003). There may be several hepcidin copies in some species (Mu et al., 2018), the reason why there were multiple hepcidin copies in some fish was not clear. It was proposed that in fish, different hepcidins may have different functions, and the additional copies may serve to support innate immunity (Hirono et al., 2005).

qRT-PCR detection illustrated that *Lc-HepL* was involved in the immune process of *C. irritans* infection, and the mRNA was significantly upregulated at different times post infection. The results were the first proof demonstrating *Lc-HepL* was involved in the anti-*C. irritans* immune response at the mRNA level. To date, reports showed many AMPs took part in the antiparasitic process, *Lc-pis* expression was significantly upregulated in all tested tissues at 6 h or one day after *C. irritans* infection, indicating that *Lc-pis* was not only constitutively expressed but also exhibited an increased response to parasite infection. Additionally, *Lc-hepc* was significantly enhanced in spleen, heart, and stomach but not in the liver and kidney after challenged by LPS (Lipopolysaccharides). Hepcidin 1 and 2 of the Japanese flounder *P. olivaceus* were induced to higher levels in liver (Hirono et al., 2005). Hepcidin in the *Lates calcarifer* was modulated in response to infection, and the most significantly up-regulated gene observed was hepcidin 1 precursor post 2 d infection when the expression level increased 91.72-fold (Khoo et al., 2012). After challenged by *C. irritans*, the increase in the liver was smaller but greater in the gill and head kidney. Therefore, the induction expression profiles of fish hepcidin caused by bacteria or *C. irritans* were significantly different.

In this study, we observed that rLc-HepL exhibited antibacterial activity to certain bacteria, including *C. glutamicum*, *M. lysodeikticus* and *P. damselae*. Compared to the antibacterial activity of Lc-hepc, rLc-HepL showed significant limitations, because

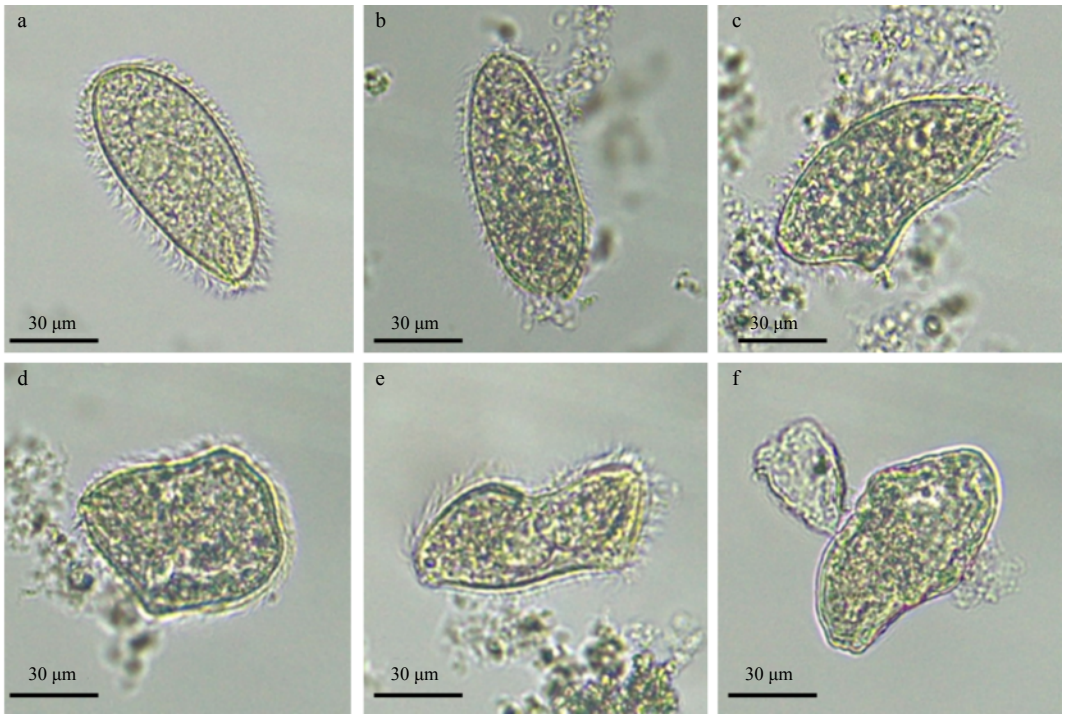

Fig. 11. Effect of 40 μmol/L rLc-HepL on the morphology of *C. irritans* theronts. The results of the light microscopy showed the dynamic changes of theronts after incubation with rLc-HepL. a. Untreated theronts; and b–f. theronts treated with rLc-HepL for 15 min (b), 30 min (c), 1 h (d), 1.5 h (e), 2 h (f), respectively.

Lc-hepc exhibited potent antibacterial activity to most of the tested Gram-positive and Gram-negative bacteria, particularly to *V. harveyi* which is a serious pathogen infecting marine fish and invertebrates (Di Pinto et al., 2008); *V. parahaemolyticus* which is an enteric pathogen typically responsible for acute human gastroenteritis associated with consuming contaminated seafood (Vizioli and Salzet, 2002); and *S. aureus* which includes resistant strains (Ruangsri et al., 2012). In Atlantic cod (*Gadus morhua*), piscidin 2 also exhibited poorer antibacterial properties than piscidin 1 due to the disrupted amphipathic structure, which is caused by the substitution of two basic residues in piscidin 1 for leucine and glycine at positions 14 and 18 (Lauth et al., 2002). Similarly, rLc-HepL showed weaker antibacterial activity than rLc-hepc, which might be the variation of phenylalanine to leucine in the mature region of Lc-HepL and lead to the instability of the disulfide linkages or even the damage of the β-sheets structure. In view of the hepcidin from different fish species, the antibacterial activity was significantly different (Balebona et al., 1998). The morphological changes of the bacteria observed with SEM in this study were similar to those described in previous Lc-hepc researches (Cai, 2010). However, we observed a large amount of floccule materials emerging at later time in our study. Because the content leakage of certain bacteria might not be sufficient to cause this phenomenon, we proposed that most of the floccule materials were likely to be secreta which were caused by rLc-HepL. In addition, Lc-hepc caused damage to the nucleus of *S. aureus*. Therefore, damaging the membrane by gathering on the membrane to a certain concentration causing holes formation, and disturbing biological processes through entering into cells were the main bactericidal mechanisms of hepcidin (Cai, 2010).

Being an antimicrobial and systemic regulator of iron homeostasis, hepcidin combats the invading pathogen by sequestering the free iron, and ultimately limits the proliferative capability of the pathogen (Nemeth et al., 2004). Regarding the antiparasitic activity, this study was the first attempt to learn the activity of hepcidin against *C. irritans*. Increasing number of studies found some AMPs were of resistance to *C. irritans* infection; therefore, they were also called antiparasitic peptides (APPs). Lc-pis was effective against *C. irritans* trophonts, killing all trophonts in a short time at 6 μmol/L. The synthetic Lc-pis-His was active against trophonts and theronts in a dose- and time-dependent manner, causing the rupture of the membrane and content leakage in both trophonts and theronts (Niu, 2013). The serum of *Siganus oramin* was found to have strong killing effect on *C. irritans*, and reversed phase high-performance liquid chromatography (RP-HPLC) was used to isolate L-amino acid oxidase-like protein (SR-LAAO) from serum that was poisonous to *C. irritans* theronts. SR-LAAO located primarily on the cell membrane and nucleus of the theronts (Wang et al., 2010, 2011), and this protein had a significantly cytotoxic effect on *C. irritans* theronts resulting in the cilia detaching from theronts, the cells becoming rounded, the membranes eventually lysing in different cell positions and the cytoplasmic contents leaking out of the cell (Li et al., 2013). The results suggested that these proteins may contribute considerably to the host non-specific immune defense mechanism to combat microbes, and have the potentials in future drug development.

References

Babitt J L, Huang F W, Wrighting D W, et al. 2006. Bone morphogenetic protein signaling by hemojuvelin regulates hepcidin expression. Nature Genetics, 38(5): 531–539, doi: 10.1038/ng1777

Balebona M C, Andreu M J, Bordas M A, et al. 1998. Pathogenicity of

Vibrio alginolyticus for cultured gilt-head sea bream (*Sparus aurata* L.). Applied and Environmental Microbiology, 64(11): 4269–4275, doi: 10.1128/AEM.64.11.4269-4275.1998

Bowdish D M E, Davidson D J, Hancock R E W. 2006. Immunomodulatory properties of defensins and cathelicidins. In: Shafer W M, ed. Antimicrobial Peptides and Human Disease. Berlin, Heidelberg: Springer, 306: 27–66

Cai Jingjing. 2010. Recombinant production, antimicrobial activity analysis and antimicrobial mechnism of hepcidin from marine fish *Pseudosciaena crocea* and *Oryzias melastigma* (in Chinese) [dissertation]. Xiamen: Xiamen University

Chen J Y, Lin Weiju, Lin Tailang. 2009. A fish antimicrobial peptide, tilapia hepcidin TH2-3, shows potent antitumor activity against human fibrosarcoma cells. Peptides, 30(9): 1636–1642, doi: 10.1016/j.peptides.2009.06.009

Destoumieux D, Bulet P, Strub J M, et al. 1999. Recombinant expression and range of activity of penaeidins, antimicrobial peptides from penaeid shrimp. European Journal of Biochemistry, 266(2): 335–346, doi: 10.1046/j.1432-1327.1999.00855.x

Di Pinto A, Ciccarese G, De Corato R, et al. 2008. Detection of pathogenic *Vibrio parahaemolyticus* in southern Italian shellfish. Food Control, 19(11): 1037–1041, doi: 10.1016/j.foodcont.2007.10.013

Douglas S E, Gallant J W, Liebscher R S, et al. 2003. Identification and expression analysis of hepcidin-like antimicrobial peptides in bony fish. Developmental & Comparative Immunology, 27(6–7): 589–601

Hirono I, Hwang J Y, Ono Y, et al. 2005. Two different types of hepcidins from the Japanese flounder *Paralichthys olivaceus*. The FEBS Journal, 272(20): 5257–5264, doi: 10.1111/j.1742-4658.2005.04922.x

Hu Xueyou, Camus A C, Aono S, et al. 2007. Channel catfish hepcidin expression in infection and anemia. Comparative Immunology, Microbiology and Infectious Diseases, 30(1): 55–69, doi: 10.1016/j.cimid.2006.10.004

Khoo C K, Abdul-Murad A M, Kua B C, et al. 2012. *Cryptocaryon irritans* infection induces the acute phase response in *Lates calcarifer*: A transcriptomic perspective. Fish & Shellfish Immunology, 33(4): 788–794

Krause A, Neitz S, Mägert H J, et al. 2000. LEAP-1, a novel highly disulfide-bonded human peptide, exhibits antimicrobial activity. FEBS Letters, 480(2–3): 147–150, doi: 10.1016/S0014-5793(00)01920-7

Lauth X, Shike H, Burns J C, et al. 2002. Discovery and characterization of two isoforms of moronecidin, a novel antimicrobial peptide from hybrid striped bass. The Journal of Biological Chemistry, 277(7): 5030–5039, doi: 10.1074/jbc.M109173200

Lauth X, Babon J J, Stannard J A, et al. 2005. Bass hepcidin synthesis, solution structure, antimicrobial activities and synergism, and *in vivo* hepatic response to bacterial infections. Journal of Biological Chemistry, 280(10): 9272–9282, doi: 10.1074/jbc.M411154200

Lee P, Peng Hongfan, Gelbart T, et al. 2005. Regulation of hepcidin transcription by interleukin-1 and interleukin-6. Proceedings of the National Academy of Sciences of the United States of America, 102(6): 1906–1910, doi: 10.1073/pnas.0409808102

Li Ruijun, Dan Xueming, Li Anxing. 2013. *Siganus oramin* recombinant L-amino acid oxidase is lethal to *Cryptocaryon irritans*. Fish & Shellfish Immunology, 35(6): 1867–1873

Livak K J, Schmittgen T D. 2001. Analysis of relative gene expression data using real-time quantitative PCR and the $2^{-\triangle\triangle CT}$ method. Methods, 25(4): 402–408, doi: 10.1006/meth.2001.1262

López-García B, Ubhayasekera W, Gallo R L, et al. 2007. Parallel evaluation of antimicrobial peptides derived from the synthetic PAF26 and the human LL37. Biochemical and Biophysical Research Communications, 356(1): 107–113, doi: 10.1016/j.bbrc.2007.02.093

Mookherjee N, Hancock R E W. 2007. Cationic host defence peptides: innate immune regulatory peptides as a novel approach for treating infections. Cellular and Molecular Life Sciences, 64(7–8): 922–933, doi: 10.1007/s00018-007-6475-6

Mu Yinnan, Huo Jieying, Guan Yanyun, et al. 2018. An improved genome assembly for *Larimichthys crocea* reveals hepcidin gene expansion with diversified regulation and function. Communication Biology, 1: 195, doi: 10.1038/s42003-018-0207-3

Nemeth E, Tuttle M S, Powelson J, et al. 2004. Hepcidin regulates cellular iron efflux by binding to ferroportin and inducing its internalization. Science, 306(5704): 2090–2093, doi: 10.1126/science.1104742

Nicholls E F, Madera L, Hancock R E W. 2010. Immunomodulators as adjuvants for vaccines and antimicrobial therapy. Annals of the New York Academy of Sciences, 1213(1): 46–61, doi: 10.1111/j.1749-6632.2010.05787.x

Niu Sufang. 2013. Study on the antiparasitic characterization of piscidin-like characterization of piscidin-like in two sciaenoid fishes (in Chinese) [dissertation]. Xiamen: Xiamen University

Oppenheim J J, Biragyn A, Kwak L W, et al. 2003. Roles of antimicrobial peptides such as defensins in innate and adaptive immunity. Annals of the Rheumatic Diseases, 62(Suppl 2): ii17–ii21

Park C H, Valore E V, Waring A J, et al. 2001. Hepcidin, a urinary antimicrobial peptide synthesized in the liver. Journal of Biological Chemistry, 276(11): 7806–7810, doi: 10.1074/jbc.M008922200

Patel S, Akhtar N. 2017. Antimicrobial peptides (AMPs): the quintessential 'offense and defense' molecules are more than antimicrobials. Biomedicine & Pharmacotherapy, 95: 1276–1283

Ruangsri J, Salger S A, Caipang C M A, et al. 2012. Differential expression and biological activity of two piscidin paralogues and a novel splice variant in Atlantic cod (*Gadus morhua* L.). Fish & Shellfish Immunology, 32(3): 396–406

Shi Jishu, Camus A C. 2006. Hepcidins in amphibians and fishes: Antimicrobial peptides or iron-regulatory hormones?. Developmental & Comparative Immunology, 30(9): 746–755

Shike H, Lauth X, Westerman M E, et al. 2002. Bass hepcidin is a novel antimicrobial peptide induced by bacterial challenge. European Journal of Biochemistry, 269(8): 2232–2237, doi: 10.1046/j.1432-1033.2002.02881.x

Shike H, Shimizu C, Lauth X, et al. 2004. Organization and expression analysis of the zebrafish hepcidin gene, an antimicrobial peptide gene conserved among vertebrates. Developmental & Comparative Immunology, 28(7–8): 747–754

Supungul P, Tang S, Maneeruttanarungroj C, et al. 2008. Cloning, expression and antimicrobial activity of crustin*Pm*1, a major isoform of crustin, from the black tiger shrimp *Penaeus monodon*. Developmental & Comparative Immunology, 32(1): 61–70

Valero Y, Saraiva-Fraga M, Costas B, et al. 2020. Antimicrobial peptides from fish: beyond the fight against pathogens. Reviews in Aquaculture, 12(1): 224–253, doi: 10.1111/raq.12314

Vizioli J, Salzet M. 2002. Antimicrobial peptides from animals: focus on invertebrates. Trends in Pharmacological Sciences, 23(11): 494–496, doi: 10.1016/S0165-6147(02)02105-3

Wang Kejiang, Cai Jingjing, Cai Lin, et al. 2009. Cloning and expression of a hepcidin gene from a marine fish (*Pseudosciaena crocea*) and the antimicrobial activity of its synthetic peptide. Peptides, 30(4): 638–646, doi: 10.1016/j.peptides.2008.12.014

Wang Fanghua, Li Ruijun, Xie Mingquan, et al. 2011. The serum of rabbitfish (*Siganus oramin*) has antimicrobial activity to some pathogenic organisms and a novel serum $_{L}$-amino acid oxidase is isolated. Fish & Shellfish Immunology, 30(4–5): 1095–1108

Wang Fanhua, Xie Mingquan, Li Anxing. 2010. A novel protein isolated from the serum of rabbitfish (*Siganus oramin*) is lethal to *Cryptocaryon irritans*. Fish & Shellfish Immunology, 29(1): 32–41

Yang Min. 2006. Cloning, expression and antimicrobial activity ana-

lysis of hepcidin gene variants in two cultured fish, *Pagrus major* and *Spagrus microcephalus* (in Chinese) [dissertation]. Xiamen: Xiamen University

Yeaman M R, Yount N Y. 2003. Mechanisms of antimicrobial peptide action and resistance. Pharmacological Reviews, 55(1): 27–55, doi: 10.1124/pr.55.1.2

Zhang Ming. 2013. Study on the functions of three immune-related genes in kuruma shrimp *Marsupenaeus japonicas* (in Chinese) [dissertation]. Xiamen: Xiamen University

Zheng Libing, Liu Zhihong, Wu Biao, et al. 2016. Ferritin has an important immune function in the ark shell *Scapharca broughtonii*. Developmental & Comparative Immunology, 59: 15–24

Zheng Libing, Mao Yong, Wang Jun, et al. 2018. Excavating differentially expressed antimicrobial peptides from transcriptome of *Larimichthys crocea* liver in response to *Cryptocaryon irritans*. Fish & Shellfish Immunology, 75: 109–114